Thermal monopole condensation and confinement in finite temperature Yang-Mills theories

Alessio D'Alessandro,[1] Massimo D'Elia,[1] and Edward V. Shuryak[2]

[1]*Dipartimento di Fisica, Università di Genova and INFN, Via Dodecaneso 33, 16146 Genova, Italy*

[2]*Department of Physics and Astronomy, State University of New York, Stony Brook, New York 11794-3800, USA*

(Received 10 March 2010; published 11 May 2010)

We investigate the connection between color confinement and thermal Abelian monopoles populating the deconfined phase of SU(2) Yang-Mills theory, by studying how the statistical properties of the monopole ensemble change as the confinement/deconfinement temperature is approached from above. In particular, we study the distribution of monopole currents with multiple wrappings in the Euclidean time direction, corresponding to two or more particle permutations, and show that multiple wrappings increase as the deconfinement temperature is approached from above, in a way compatible with a condensation of such objects happening right at the deconfining transition. We also address the question of the thermal monopole mass, showing that different definitions give consistent results only around the transition, where the monopole mass goes down and becomes of the order of the critical temperature itself.

DOI: 10.1103/PhysRevD.81.094501 PACS numbers: 11.15.Ha, 64.60.Bd, 12.38.Aw, 67.85.Jk

I. INTRODUCTION

Color confinement is not yet fully understood in terms of the first principles of quantum chromodynamics (QCD). Models exist which relate confinement to the condensation of topological defects in the QCD ground state; one of them is based on dual superconductivity of the QCD vacuum [1,2]. According to this model, color confinement is due to the spontaneous breaking of a magnetic symmetry, induced by the condensation of magnetically charged objects (e.g. magnetic monopoles), which yields a nonvanishing magnetically charged Higgs condensate.

The existence of a new phase of matter, in which quark and gluons are deconfined (quark-gluon plasma), is a well-defined prediction of lattice QCD simulations: the deconfined phase is under active experimental search in heavy ion experiments. However, the physical properties expected for this phase are not yet clearly understood: the quark-gluon plasma is still strongly interacting above the deconfining temperature T_c, and its properties may be more similar to those of an almost perfect liquid.

One of the hypotheses which have been put forward in the recent past is that quark-gluon plasma properties may be dominated by a magnetic component [3–5]. In Ref. [4] such magnetic component has been related to thermal Abelian monopoles evaporating from the magnetic condensate which is believed to induce color confinement at low temperatures; moreover, it has been proposed to detect such thermal monopoles in finite temperature lattice QCD simulations, by identifying them with monopole currents having a nontrivial wrapping in the Euclidean temporal direction [4,6,7]. First numerical investigations of these wrapping trajectories were performed in Refs. [6,7], while a systematic study, regarding the deconfined phase of SU(2) Yang-Mills theory, has been performed in Ref. [8].

The definition of Abelian magnetic monopoles in non-Abelian gauge theories requires the identification of Abelian degrees of freedom: that is done usually by a procedure known as Abelian projection and relies on the choice of an adjoint field. Since no natural adjoint field exists in usual QCD, that implies some arbitrariness; a popular choice is to perform the projection in the so-called maximal Abelian gauge (MAG). Results obtained in Ref. [8] have shown that, as already well known for Abelian monopole currents in general, also the number and the locations of monopole currents with a nontrivial wrapping in the Euclidean time direction are quantities which depend on the choice of the Abelian projection.

Despite that, the density and the spatial correlation functions of MAG thermal monopoles show a negligible dependence on the UV cutoff [8], as expected for a physical quantity. The temperature dependence of the monopole density, ρ, is not compatible with a (massive or massless) free particle behavior and is instead well described, in the whole range of temperatures explored, by a behavior $\rho \propto T^3/(\log T/\Lambda_{\rm eff})^2$ with $\Lambda_{\rm eff} \sim 100$ MeV, while the behavior $\rho \propto T^3/(\log T)^3$, predicted by dimensional reduction arguments, is compatible with data for $T > 5T_c$. This is in agreement with the picture of an electric dominated phase for Yang-Mills theories at very high temperatures, in which the magnetic component is strongly interacting [3].

Moreover, the study of density-density spatial correlation functions has verified the presence of a repulsive (attractive) interaction for a monopole-monopole (monopole-antimonopole) pair, which at large distances is in agreement with a screened Coulomb potential and a screening length of the order of 0.1 fm. The above results have suggested a liquid-like behavior for the thermal monopole ensemble above T_c [9] and stimulated further research about the possible role of magnetic monopoles in the quark-gluon plasma [10–12].

In the present paper, while aware of the problems related to the definition of thermal Abelian monopoles, we work on the hypothesis that those defined in the MAG may have

a physical meaning (we will discuss further about this point in Sec. V) and address a question regarding color confinement: if thermal monopoles in the deconfined phase are really related to the magnetic condensate responsible for confinement below the deconfinement temperature, $T < T_c$, is it possible to find clear signatures for their approach to condensation for temperatures slightly above T_c? Such an approach would complement standard studies about the validity of the dual superconductor model, which look at the spontaneous breaking of a magnetic symmetry in the confined phase (i.e. the presence of a magnetic condensate) and at its restoration as T_c is approached from below [13–20].

Since condensation is a phenomenon strictly related to quantum statistics, any signal of it should be searched for in properties of thermal Abelian monopole trajectories which reflect their nature of identical quantum objects. Such properties, as better explained in the following, are encoded in monopole trajectories which wrap two or more times in the Euclidean time direction and correspond to the permutation of two or more particles: no or very few multiple wrapping trajectories are expected if the system is very close to the Boltzmann approximation, while their number should increase as quantum effects become important, in a critical way close to the point where the particles condense. Such an approach goes back to the seminal papers by Feynman [21,22], where a path integral formulation was applied to describe condensation phenomena like the superfluid transition in ^{4}He. Since then, the path integral formulation of multiparticle systems has become an invaluable tool for analytical and numerical investigations of Bose condensation [23,24], and has been recently reconsidered in Ref. [25], where it has been suggested to apply it also to the analysis of monopole condensation in QCD.

A second question that we address regards the mass of thermal monopoles. Different strategies can be followed to determine some temperature dependent effective mass. For instance, one can look at the effective mass appearing in the description of multiply wrapping trajectories above T_c or, in close analogy with the path integral formulation for nonrelativistic quantum particles, one can obtain information about the mass by looking at the spatial fluctuations of wrapping trajectories. Of course it is not guaranteed that different strategies will lead to consistent determinations.

The paper is organized as follows. In Sec. II we recall a few technical details about the definition of thermal Abelian monopoles on the lattice. In Sec. III we study the distribution of multiply wrapping monopole trajectories in the deconfined phase of the SU(2) pure gauge theory and give an interpretation of them in terms of monopole condensation, determing a condensation temperature which is consistent with the known deconfinement temperature T_c. In Sec. IV we address the question of the monopole mass. Finally, in Sec. V, we discuss our results and draw our conclusions.

II. ABELIAN PROJECTION AND THERMAL MONOPOLES ON THE LATTICE

The definition of Abelian monopoles requires the identification of a U(1) subgroup of the original gauge group. This is done by a procedure known as Abelian projection, which is assigned in terms of an adjoint field, i.e., in the particular case of SU(2) color gauge group, a vector field $\vec{\phi}(x)$ transforming as

$$\vec{\sigma}\cdot\vec{\phi}(x) \to G(x)(\vec{\sigma}\cdot\vec{\phi}(x))G^\dagger(x) \tag{1}$$

under a local gauge transformation $G(x)$ ($\vec{\sigma}$ denote Pauli matrixes). If $\vec{G}_{\mu\nu}(x)$ is the field strength tensor of the original SU(2) gauge theory, then an Abelian tensor, known as 't Hooft tensor, is defined in terms of $\vec{\phi}(x)$

$$\begin{aligned} F_{\mu\nu} &= \hat{\phi}\cdot\vec{G}_{\mu\nu} - \frac{1}{g}\hat{\phi}\cdot(D_\mu\hat{\phi}\wedge D_\nu\hat{\phi}) \\ &= \partial_\mu(\hat{\phi}\cdot\vec{A}_\nu) - \partial_\nu(\hat{\phi}\cdot\vec{A}_\mu) - \frac{1}{g}\hat{\phi}\cdot(\partial_\mu\hat{\phi}\wedge\partial_\nu\hat{\phi}), \end{aligned} \tag{2}$$

where $\hat{\phi}(x) \equiv \vec{\phi}(x)/|\vec{\phi}(x)|$. $F_{\mu\nu}$ is an Abelian, gauge independent tensor, which in the gauge where $\hat{\phi}(x) = (0, 0, 1)$ takes the form

$$F_{\mu\nu} = \partial_\mu A^3_\nu - \partial_\nu A^3_\mu.$$

In that gauge, which is fixed up to a U(1) residual gauge freedom [$\hat{\phi} \in SO(3)/\mathrm{U}(1)$], the Abelian projection corresponds to taking the diagonal part of gauge links.

In usual QCD there is no natural adjoint field, but several adjoint fields can be constructed in terms of gauge fields, typically a closed parallel transport (i.e. a path ordered product of gauge links). Alternatively, an implicit definition can be assigned by fixing $\hat{\phi} = (0, 0, 1)$ and constant in one particular gauge: that defines $\hat{\phi}(x)$ in every other gauge. An example is the so-called maximal Abelian gauge, where the gauge is fixed by maximizing the following functional with respect to gauge transformations:

$$F_{\mathrm{MAG}} = \sum_{\mu,n}\mathrm{Re}\,\mathrm{tr}[U_\mu(n)\sigma_3 U^\dagger_\mu(n)\sigma_3], \tag{3}$$

where $U_\mu(n)$ is a non-Abelian gauge link variable, i.e. an elementary parallel transport from lattice site n to $n + \hat{\mu}$. F_{MAG} is proportional to the average squared diagonal part of the gauge links.

In the gauge where the 't Hooft tensor is diagonal, Abelian link phases are extracted as follows:

$$\begin{aligned} U_\mu(n) &= u^0_\mu\mathrm{Id} + i\vec{\sigma}\cdot\vec{u}_\mu \to \mathrm{diag}(e^{i\theta_\mu(n)}, e^{-i\theta_\mu(n)}) \\ &\equiv \frac{(u^0_\mu\mathrm{Id} + i\sigma_3 u^3_\mu)}{\sqrt{(u^0_\mu)^2 + (u^3_\mu)^2}}. \end{aligned} \tag{4}$$

Abelian plaquettes, i.e. the lattice discretization of the

't Hooft field strength tensor, can then be constructed starting from the Abelian gauge link phases $\theta_\mu(n)$:

$$\theta_{\mu\nu} \equiv \theta_\mu(n) + \theta_\nu(n+\hat{\mu}) - \theta_\mu(n+\hat{\nu}) - \theta_\nu(n) \equiv \hat{\partial}_\mu \theta_\nu - \hat{\partial}_\nu \theta_\mu. \quad (5)$$

Of course, Abelian plaquettes can be extracted also in a gauge where $\hat{\phi}(x)$ is not constant, even if through a more intricate procedure [26], obtaining equivalent results [26,27], as expected from the gauge invariance of 't Hooft tensor.

Abelian monopole currents are identified by the standard De Grand-Toussaint construction [28]:

$$m_\mu = \frac{1}{2\pi} \varepsilon_{\mu\nu\rho\sigma} \hat{\partial}_\nu \bar{\theta}_{\rho\sigma}, \quad (6)$$

where $\bar{\theta}_{\rho\sigma}$ is the compactified part of the Abelian plaquette phase

$$\theta_{\mu\nu} = \bar{\theta}_{\mu\nu} + 2\pi n_{\mu\nu} \quad (7)$$

and $n_{\mu\nu} \in \mathbf{N}$.

Monopole currents form closed loops, since $\hat{\partial}_\mu m_\mu = 0$. These loops may be either topologically trivial or wrapped around the lattice. Following the proposal of Ref. [4], among the different currents, we select those having a nontrivial positive (negative) wrapping around the Euclidean temporal direction, identifying them with thermal monopoles (antimonopoles).

This procedure identifies, at any given time slice, the spatial positions of thermal monopoles with the points pierced by a current with nontrivial wrapping. There is some sort of ambiguity in this identification, since monopole currents extracted on the lattice are not strictly one-dimensional objects, but rather clusters of currents becoming approximately one-dimensional tubes in the high temperature phase, but staying anyway of finite thickness in lattice spacing units, because of UV noise which is present in the form of small monopole loops attached to the wrapping current. In our numerical setup we fix the spatial position of the monopole at the point where the wrapping monopole current is first detected by the current searching algorithm: thermal monopoles are thus spatially located with some random noise, which however has negligible systematic effects on the density and spatial correlation functions of thermal monopoles.

Some of the monopole currents may wrap more than once, say k times, in the Euclidean time direction: in this case, as better explained in the following, we interpret them as sets of k monopoles (or antimonopoles) undergoing a cyclic permutation after a wrap in Euclidean time. The density and distribution of those k times wrapping trajectories is one of the subject of the present investigation. Also in this case, mainly due to the finite thickness of the wrapping current induced by UV fluctuations, ambiguities may be present for some specific configurations. One can imagine of situations in which it is hard to distinguish between two currents, each wrapping once, and a single current with a double wrap: that may happen, for instance, if the two currents overlap in some point and the answer may depend on the algorithm used to follow the current around the lattice. In our measurements we have chosen different current searching algorithms, and we have taken the discrepancies between the different algorithms as an estimate of the systematic error linked to such ambiguities: such systematic error is always included in our determinations.

In the following we shall present results obtained in the maximal Abelian gauge. It can be shown that, on stationary points of the MAG functional, the local operator

$$X(n) = \sum_\mu [U_\mu(n)\sigma_3 U_\mu^\dagger(n) + U_\mu^\dagger(n-\hat{\mu})\sigma_3 U_\mu(n-\hat{\mu})] \quad (8)$$

is diagonal. The maximization of the MAG functional for a given configuration has been achieved by an iterative combination of local maximization and overrelaxation (see Ref. [29]), stopping the algorithm when the average squared modulus of the nondiagonal part of $X(n)$ was less than a given parameter ω [29]. We have chosen $\omega = 10^{-8}$ (see Ref. [8] for more details).

III. MONOPOLE CONDENSATION

If we interpret the set of wrapping monopole trajectories, extracted from one gauge configuration of our Monte-Carlo sample, as one possible configuration of the Euclidean path integral representation of an ensemble of identical monopoles and antimonopoles at thermal equilibrium, then a trajectory which wraps k times before closing can be interpreted as a set of k monopoles (or antimonopoles) which permutate cyclically after going through the periodic Euclidean time direction.

In the path integral describing N identical particles at thermal equilibrium, each possible configuration of the N particle paths contributing to the functional integral needs

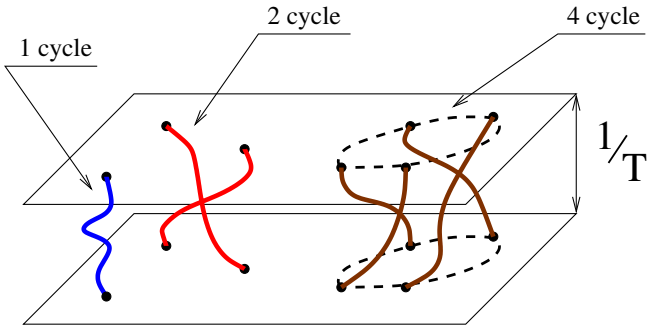

FIG. 1 (color online). A possible contribution to the path integral representation of the partition function of 7 identical particles, in which the particles undergo a permutation made up of a 1 cycle, a 2 cycle, and a 4 cycle.

TABLE I. Normalized average densities ρ_k/T^3 of trajectories wrapping k times, as a function of T/T_c for SU(2) pure gauge theory. The superscript a or b above the temperature value refers to two different values of the lattice spacing, 0.047 fm and 0.063 fm, respectively. Blank spaces indicate that no monopole current with the given wrapping has been observed in our statistical sample.

T/T_c	ρ_1/T^3	ρ_2/T^3	ρ_3/T^3	ρ_4/T^3	ρ_5/T^3	ρ_6/T^3	ρ_7/T^3	ρ_8/T^3
1.017^a	0.308(2)	$1.53(1)\ 10^{-2}$	$3.40(5)\ 10^{-3}$	$1.21(3)\ 10^{-3}$	$4.1(3)\ 10^{-4}$	$2.0(3)\ 10^{-4}$	$0.6(2)\ 10^{-4}$	$2.4(5)\ 10^{-5}$
1.052^b	0.315(5)	$1.35(1)\ 10^{-2}$	$2.42(4)\ 10^{-3}$	$7.0(2)\ 10^{-4}$	$2.5(2)\ 10^{-4}$	$8.2(5)\ 10^{-5}$	$3.6(5)\ 10^{-5}$	$1.1(3)\ 10^{-5}$
1.095^a	0.3395(15)	$1.23(2)\ 10^{-2}$	$1.81(5)\ 10^{-3}$	$4.1(4)\ 10^{-4}$	$0.9(1)\ 10^{-4}$	$2.3(5)\ 10^{-5}$	$1.0(5)\ 10^{-5}$	
1.168^b	0.325(3)	$8.0(1)\ 10^{-3}$	$7.6(2)\ 10^{-4}$	$1.2(1)\ 10^{-4}$	$1.1(3)\ 10^{-5}$	$0.2(1)\ 10^{-5}$		
1.187^a	0.337(2)	$8.1(1)\ 10^{-3}$	$7.3(4)\ 10^{-4}$	$1.1(1)\ 10^{-4}$	$1.5(4)\ 10^{-5}$	$0.4(2)\ 10^{-5}$		
1.295^a	0.316(1)	$4.72(10)\ 10^{-3}$	$2.6(3)\ 10^{-4}$	$2.0(6)\ 10^{-5}$	$0.3(2)\ 10^{-5}$			
1.315^b	0.297(2)	$3.83(3)\ 10^{-3}$	$1.7(1)\ 10^{-4}$	$1.3(2)\ 10^{-5}$	$0.6(3)\ 10^{-6}$			
1.424^a	0.286(1)	$2.52(5)\ 10^{-3}$	$8.4(7)\ 10^{-5}$	$0.4(2)\ 10^{-5}$				
1.503^b	0.271(1)	$1.78(5)\ 10^{-3}$	$4.1(3)\ 10^{-5}$	$0.8(4)\ 10^{-6}$				
1.582^a	0.252(1)	$1.28(2)\ 10^{-3}$	$2.5(3)\ 10^{-5}$	$1.0(5)\ 10^{-6}$				
1.754^b	0.2134(10)	$7.3(3)\ 10^{-4}$	$9(1)\ 10^{-6}$	$0.2(1)\ 10^{-6}$				
1.780^a	0.2190(2)	$6.26(7)\ 10^{-4}$	$8.3(8)\ 10^{-6}$	$0.2(1)\ 10^{-6}$				
2.034^a	0.1870(4)	$3.04(10)\ 10^{-4}$	$1.0(4)\ 10^{-6}$					
2.105^b	0.1745(10)	$3.02(20)\ 10^{-4}$	$1.7(4)\ 10^{-6}$					
2.373^a	0.1574(4)	$1.30(6)\ 10^{-4}$	$0.4(2)\ 10^{-6}$					
2.631^b	0.1410(10)	$1.30(10)\ 10^{-4}$	$0.3(1)\ 10^{-6}$					
2.848^a	0.1306(4)	$6.3(2)\ 10^{-5}$	$0.2(1)\ 10^{-6}$					
3.560^a	0.1073(3)	$3.3(4)\ 10^{-5}$	$0.4(4)\ 10^{-7}$					

to be periodic, apart from a possible permutation of the N particles (the sign of the permutation is attached to the contribution if the particles are fermions). That means that the configuration is not necessarily composed of N closed paths (that would correspond to the identical permutation), but is in general made up of M closed paths, with $M \leq N$: if the jth path wraps k_j times around the Euclidean time direction, then $\sum_{j=1}^{M} k_j = N$ and the configuration corresponds to a permutation made up of M cycles of sizes $k_1, k_2, \ldots, k_M$. In Fig. 1 we report an example corresponding to a permutation of 7 particles partitioned into a 1 cycle, a 2 cycle, and a 4 cycle.

If effects related to quantum statistics are negligible, i.e. if the system is very close to the Boltzmann approximation, configurations corresponding to permutations different from the identical one are expected to have a negligible weight in the path integral, so that trajectories wrapping more than one time, corresponding to the exchange of two or more particles, are very rare. The number of trajectories wrapping more and more times is instead expected to increase as quantum effects become more important, and this should be especially true close to a transition associated with Bose-Einstein condensation (BEC) (or with similar phenomena).

A. Numerical simulations

In Table I we report the normalized average densities ρ_k/T^3 of trajectories wrapping k times as a function of temperature, determined for SU(2) pure gauge theory by use of the standard plaquette action and of the MAG Abelian projection. Data include both monopole and antimonopole trajectories and have been obtained by extracting monopole currents from samples consisting of $O(10^3)$ independent gauge configurations for each value of T. The superscript a or b above the temperature value refers to two different values of the inverse gauge coupling, $\beta = 2.70$ and $\beta = 2.60$, corresponding, respectively, to lattice spacings $a(\beta) \simeq 0.047$ fm and $a(\beta) \simeq 0.063$ fm.[1] Simulations have been done at fixed spatial volume, while the temperature $T = 1/(N_t a(\beta))$ has been changed by varying the number of lattice sites N_t in the temporal direction. In particular, at $\beta = 2.70$ we have made simulations on $64^3 \times N_t$ lattices, with $N_t = 4, 5, \ldots, 14$, while at $\beta = 2.60$ we have chosen $48^3 \times N_t$ lattices, with $N_t = 4, 5, \ldots, 10$. Different spatial volumes have been considered in some cases for $\beta = 2.60$, in order to check for finite size effects. Confirming results reported for the overall monopole-antimonopole density in Ref. [8], data obtained for each ρ_k show a reasonable independence from the value of the UV cutoff, even if small deviations are visible.

Numerical data for ρ_k/T^3 are also reported in Fig. 2. What is apparent from the figure is that the relative weight of trajectories wrapping more than one time increases rapidly as T approaches T_c from above. The number of monopoles or antimonopoles which are found in nontrivial cycles (i.e. $k > 1$) is less than 0.1% for $T > 2.5T_c$, meaning

[1]The physical scale has been determined according to $a(\beta)\Lambda_L = R(\beta)\lambda(\beta)$, where R is the two-loop perturbative β function, while λ is a nonperturbative correction factor computed and reported in Ref. [30]. We have assumed the values $T_c/\Lambda_L = 21.45(14)$ [30], $T_c/\sqrt{\sigma} = 0.69(2)$ [31], and $\sqrt{\sigma} \simeq 430$ MeV.

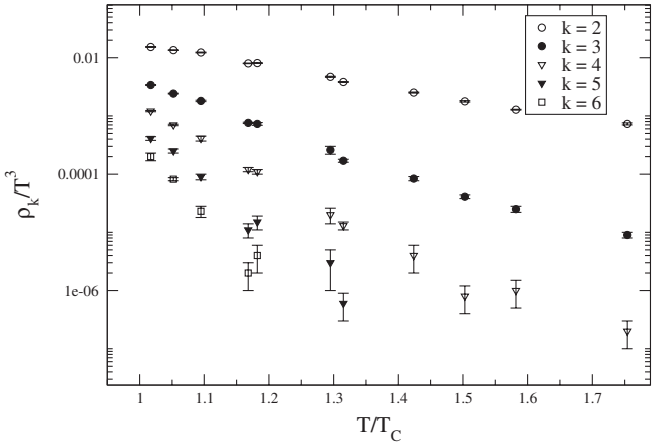

FIG. 2. Normalized densities ρ_k/T^3 as a function of T/T_c.

that the system is essentially Boltzmann-like at high temperatures. The same number goes to about 1% for $T \sim 1.5T_c$ and is well above 10% at the lowest temperature explored in our simulations.

This is a clear qualitative signature for quantum statistics effects becoming more and more relevant as the critical temperature is approached, as expected if monopoles condense at T_c. In the following we shall try to be more quantitative, but in order to do that we need to rely on some specific model. We shall first consider the analysis of a system of nonrelativistic noninteracting bosons, following what performed in Refs. [22,23] as a starting point to describe the transition to superfluid helium. We shall then discuss the deviations from this very simple model which are expected for the monopole-antimonopole ensemble in QCD.

B. Noninteracting Model for BEC

We consider a system of N identical bosonic particles and their partition function $Z = \mathrm{Tr}(e^{-H/T})$. The trace can be taken over position eigenstates $|x_1 \cdots x_N\rangle$, but the correct states to consider in case of identical particles are proportional[2] to

$$\sum_P |x_{P_1} \ldots x_{P_N}\rangle,$$

where the sum is over all the possible permutations P of the N particles. The partition function can be written as

$$Z = \frac{1}{N!}\sum_P \int d^3x_1 \ldots \int d^3x_N \langle x_{P_1} \ldots x_{P_N}|e^{-\beta H}|x_1 \ldots x_N\rangle. \tag{9}$$

We keep only the kinetic term $K = p^2/(2m)$ of the Hamiltonian H, discarding interactions and relativistic effects: we shall discuss these approximations in Sec. III C.

The assumption of absence of particle-particle interactions implies that the matrix element in Eq. (9) can be conveniently factorized according to the decomposition of the permutation into disjoint cycles. To clarify this point, consider the following explicit case involving 5 particles and a permutation composed of a 3 cycle plus a 2 cycle:

$$\begin{aligned}\langle x_3, x_1, x_2, x_5, x_4|e^{-H/T}|x_1, x_2, x_3, x_4, x_5\rangle \\ = \langle x_3, x_1, x_2|e^{-(p_1^2+p_2^2+p_3^2)/(2mT)}|x_1, x_2, x_3\rangle \\ \times \langle x_5, x_4|e^{-(p_4^2+p_5^2)/(2mT)}|x_4, x_5\rangle.\end{aligned} \tag{10}$$

Also, the integration in Eq. (9) can be carried on independently over groups of x variables belonging to the same cycle, so that each summand permutation can be factorized into a product of different contributions and the partition function can be rewritten as follows:

$$Z = \frac{1}{N!}\sum_P \prod_k z_k^{n_k}, \tag{11}$$

where

$$\begin{aligned}z_k \equiv \int d^3y_1 \cdots \int d^3y_k \langle y_2, y_3 \cdots y_k, y_1 \\ \times |e^{-(p_1^2+\cdots+p_k^2)/(2mT)}|y_1, y_2 \cdots y_k\rangle\end{aligned} \tag{12}$$

is the contribution coming from one k cycle and n_k is the number of different k cycles appearing in the cycle decomposition of the permutation P. It is straightforward to see that z_k can be rewritten as

$$\begin{aligned}z_k(T) = \int d^3y_1 \cdots \int d^3y_k \langle y_1|e^{-(p_k^2/2mT)}|y_k\rangle \\ \cdots \langle y_3|e^{-(p_2^2/2mT)}|y_2\rangle\langle y_2|e^{-(p_1^2/2mT)}|y_1\rangle \\ = \int d^3y_1 \langle y_1|e^{-k(p^2/2mT)}|y_1\rangle = z_1(T/k),\end{aligned} \tag{13}$$

where $z_1(T/k)$ is the partition function for a single particle at a temperature k times lower. Notice that the whole derivation would be unchanged if the particles move in an external potential, but still in absence of particle-particle interactions.

The partition function for a nonrelativistic free particle in a box is well known:

$$z_1(T) = V/\lambda^3, \tag{14}$$

where V is the available volume and $\lambda = \sqrt{2\pi/(mT)}$ is the De Broglie thermal wavelength. There is an approximation involved in the result above: the spacing between the quantum energy levels of the particle must be negligible with respect to T, so that the sum over energy levels can be replaced by an integral. That condition can be written equivalently, for a cubic box, as $\lambda \ll V^{1/3}$, i.e. the thermal wavelength must be negligible with respect to the size of

[2]The normalization factor is $1/\sqrt{N!}$ if the N coordinates are all different and changes otherwise.

the box; a similar condition applies if the particle is constrained in a three-dimensional periodic torus, as happens in our lattice setup. For a given volume, this condition is violated at low enough temperatures.

Combining Eqs. (13) and (14), we obtain

$$z_k(T) = z_1(T/k) = \frac{V}{\lambda^3 k^{3/2}}, \tag{15}$$

but the condition for its validity is now $\sqrt{k}\lambda \ll V^{1/3}$. Such condition can be violated, for given V and T, if k is large enough. To better understand this condition, think of the loop constructed with the positions of the k particles belonging to the cycle; the integral in Eq. (12) can be rewritten in terms of integration over the relative coordinates of neighboring particles plus an integration over the center of mass of the loop: only if the size of the loop, which is of order $\sqrt{k}\lambda$, is negligible with respect to the size of the box, the integration over the center of mass can be approximated by V.

In the following we shall substitute Eq. (15) into Eq. (11), assuming that the contribution from permutations having very large cycles is suppressed: that coincides with the approximation made in Ref. [23]. The approximation is expected to work well, apart from very close to the condensation temperature. Data reported in Table I give us the opportunity to check directly if this assumption is reasonable for our ensemble of monopole trajectories. We see that indeed large values of k are exponentially suppressed, so that only cycles with small k can be found, apart from very close to T_c. Therefore we shall assume the validity of Eq. (15), being aware that violations are expected close to T_c: such violations are part of the finite size effects arising close to a critical point.

With the assumption above, the partition function in Eq. (11) becomes

$$\begin{aligned} Z &= \frac{1}{N!}\sum_P \prod_k \left(\frac{V}{\lambda^3}\frac{1}{k^{3/2}}\right)^{n_k} \\ &= \sum_{n_1,n_2\ldots n_N} \frac{1}{N!} C(n_1, n_2 \cdots n_N) \prod_k \left(\frac{V}{\lambda^3}\frac{1}{k^{3/2}}\right)^{n_k}, \end{aligned} \tag{16}$$

where we made explicit the partition into cycles (n_1 1 cycles, n_2 2 cycles, …, n_k k cycles) of each permutation P. The factor $C(n_1, n_2 \cdots n_N)$ accounts for the multiplicity of each partition $\{n_1, n_2 \cdots n_N\}$:

$$C(n_1, n_2 \cdots n_N) = \frac{N!}{1^{n_1} 2^{n_2} \cdots n_1! n_2! \cdots}, \tag{17}$$

as it follows from a simple calculation.

The exact computation of the sum in (16) is not simple, due to the presence of the constraint $\sum_k k n_k = N$ on the possible partitions, which must sum up to the total number of particles. This difficulty can be avoided by relaxing the constraint, i.e. by switching to the grand canonical formalism. The grand canonical partition function, $\mathcal{Z} \equiv \mathrm{Tr}(e^{-(H-\mu N)/T})$, can be easily computed starting from Eqs. (16) and (17):

$$\begin{aligned} \mathcal{Z} &= \sum_{n_1,n_2\cdots} \frac{\exp(\frac{\mu}{T}\sum_k k n_k)}{1^{n_1} 2^{n_2} \cdots n_1! n_2! \cdots} \prod_k \left(\frac{V}{\lambda^3}\frac{1}{k^{3/2}}\right)^{n_k} \\ &= \prod_k \exp\left(\frac{V e^{\mu k/T}}{\lambda^3 k^{5/2}}\right) \end{aligned} \tag{18}$$

and from the grand canonical partition function the average density of k cycles easily follows:

$$\rho_k \equiv \frac{\langle n_k \rangle}{V} = \frac{e^{-\hat{\mu} k}}{\lambda^3 k^{5/2}}, \tag{19}$$

where we have defined the dimensionless chemical potential $\hat{\mu} \equiv -\mu/T$, which satisfies the constraint $\hat{\mu} \geq 0$ (i.e. $\mu \leq 0$).

The expression for the total particle density is then

$$\frac{N}{V} \simeq \rho = \sum_{k=1}^{\infty} k\rho_k = \frac{1}{\lambda^3}\sum_{k=1}^{\infty} \frac{e^{-\hat{\mu} k}}{k^{3/2}}. \tag{20}$$

Of course, the last expression must be equal to the usual result for the density of an ideal nonrelativistic boson gas which is obtained when working in momentum space: that can be easily verified by recalling one of the integral expressions for the polylogarithm $\mathrm{Li}_s(z) = \sum_k z^k/k^s$, in our case in particular:

$$\sum_k \frac{e^{-\hat{\mu} k}}{k^{3/2}} = \frac{2}{\sqrt{\pi}} \int_0^{\infty} dx \frac{\sqrt{x}}{e^{\hat{\mu}} e^x - 1}. \tag{21}$$

The expression for the total density is bounded by an upper limit which is reached for $\hat{\mu} = 0$

$$\rho_{\max} = \frac{1}{\lambda^3}\sum_{k=1}^{\infty} \frac{1}{k^{3/2}} \simeq \frac{2.612}{\lambda^3}. \tag{22}$$

For larger densities or, at a fixed density, for lower temperatures (larger λ) our description is inadequate and it is necessary to allow for macroscopic cycles or equivalently, when working in momentum space, for a macroscopic number of particles occupying the ground (zero momentum) state: that corresponds to Bose-Einstein condensation. The critical temperature (density) is signalled by the vanishing of the chemical potential.

If we had a set of trajectories in configuration space sampled from the path integral representation of an ideal nonrelativistic Bose-Einstein gas at various different temperatures, we could measure the distribution of k cycles, i.e. the densities ρ_k, and then, by fitting the expected dependence given in Eq. (19), we could determine the chemical potential $\hat{\mu}$ as a function of T, in order to find numerically the critical temperature T_{BEC} at which $\hat{\mu}$ vanishes and Bose-Einstein condensation begins.

The advantage of treating the condensation of the ideal gas in configuration space rather than in momentum space

should be obvious at this stage: we have a direct connection with the information about the monopole ensemble which can be retrieved by lattice QCD simulations. The aim of our analysis is indeed to try a similar thing with our ensemble of monopole trajectories, i.e. to determine if some critical temperature $T_{\rm BEC}$ exists at which the analogous of the chemical potential vanishes, and what is its relation with the deconfinement temperature T_c. There are of course various caveats related to particle-particle interactions, that we shall discuss in the next subsection.

C. BEC of thermal monopoles

The ensemble of thermal Abelian monopoles that we are investigating is surely different from an ideal gas of nonrelativistic identical particles. The analysis of Ref. [8] indeed has shown the presence of particle-particle interactions, which are attractive in the monopole-antimonopole case and repulsive in the monopole-monopole case. The presence of those interactions interferes with many steps of the above derivation for the densities ρ_k; for instance, it is not possible to rewrite the contribution of a single k cycle as in Eq. (13).

One of the effects of interactions is visible in the particle density around a given thermal monopole, which is suppressed (enhanced) for monopoles (antimonopoles) with respect to the average density. In the monopole-monopole case the suppression extends, close to T_c, over distances of the order of 1 fm: as we shall discuss in the next section, such distance is larger than the typical thermal wavelength λ which can be measured on trajectories wrapping only one time. As a consequence, interactions should clearly affect monopole trajectories corresponding to k cycles with $k > 1$; the typical size of these loops should be $\lambda\sqrt{k}$ in the noninteracting case, but is expected to be larger due to monopole-monopole repulsion: that corresponds indeed to the outcome of the analysis to be presented in the next section.

Apart from the interactions among particles belonging to the same loop, one should also take into account loop-loop interactions, which can be both repulsive or attractive [a monopole k cycle will repel (attract) a monopole (antimonopole) k' cycle], so that it is also not possible to factorize the contribution of each permutation into the contribution of different k cycles, as in Eq. (11).

Even if we have some partial information about interactions from the analysis of Ref. [8], taking them properly into account, in order to repeat the description of BEC along the same lines reported above for the free case, is not an easy task.

Instead of looking for an exact solution, let us try to understand which similarities and differences should be expected for the dependence of the density ρ_k on k, with respect to the free case reported in Eq. (19). On general grounds, one may expect some finite free energy cost needed to add one particle to a k cycle, i.e. to go from k to $k+1$, playing the role of an effective chemical potential, plus some interaction dependent contribution, so that

$$\rho_k = e^{-\hat{\mu}k} f(k), \tag{23}$$

where $f(k)$ is some function decreasing less than exponentially with k. We shall refer to $\hat{\mu}$ as chemical potential in the following; however, it should be clear that in the present context, in which we are dealing with a neutral plasma of monopoles and antimonopoles, it should be better regarded as a parameter for an effective description of the distribution in the number of k cycles.

The result obtained in the free case, $f(k) = (\lambda^3 k^{5/2})^{-1}$, can be modified by interactions in various ways. In the case of a dilute hard sphere gas model, reported in Ref. [23], $f(k)$ is the same as in the free case plus corrections of order r/λ, where r is the sphere radius. Part of the interactions could be also taken into account by an effective dynamical mass, as done by Feynman for the study of ^{4}He. In general we may expect a leading contribution $f(k) \propto 1/k^\alpha$, where α could be different from $5/2$ (this is also the way in which relativistic effects should show up). In any case, the approach to condensation should be signalled by the vanishing of the chemical potential, i.e. at the condensation point large k cycles should cease to be suppressed exponentially in k. This is exactly what we want to check on our data reported in Table I. As we shall discuss soon, the outcome is that the vanishing of the chemical potential happens at a point which is compatible with T_c and that this result is remarkably stable for various different choices of the function $f(k)$.

We have tried to fit our data for the normalized densities ρ_k/T^3 according to $Ae^{-\hat{\mu}k}/k^\alpha$. In order to obtain reasonable values for χ^2/d.o.f., we had to take into account only data with $k > 2$–3 for $T \leq 1.2T_c$ and with $k > 1$ for higher temperatures. If the α parameter is left free, the χ^2 is minimized for α around 2 for most of the explored temperatures; however, reasonable fits are obtained for a larger range of α values.[3] A few examples of such fits are shown in Fig. 3, while in Table II we report results obtained for the chemical potential for various values of α going from 0 to 3.

As a second step, we have tried to fit the values obtained for the chemical potential according to a critical behavior:

$$\hat{\mu} = A(T - T_{\rm BEC})^{\nu'} \tag{24}$$

which predicts $\hat{\mu}$ to vanish, as the condensation temperature $T_{\rm BEC}$ is approached from above, with a critical exponent ν'. Such functional dependence describes reasonably well data reported in Table II, for each different value of α, if the lowest temperature, $T = 1.017T_c$, is discarded: this

[3]Notice that a value $\alpha > 2$ is to be preferred for the asymptotic large k behavior, since in this case the total number of particles $\sum k\rho_k$ is convergent even for $\hat{\mu} = 0$, thus claiming for a macroscopic number of particles occupying the ground state.

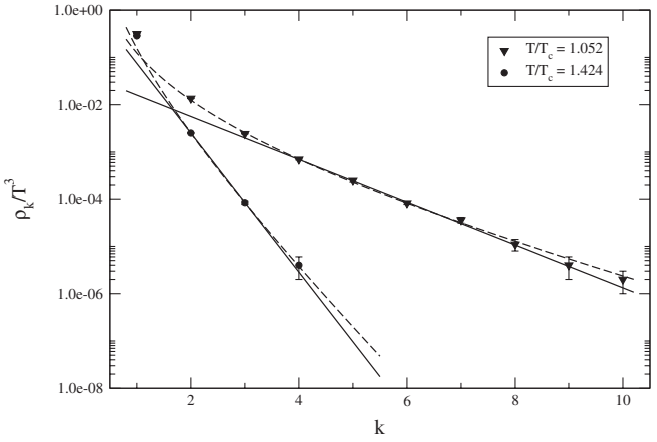

FIG. 3. Fit of the densities ρ_k according to $e^{-\hat{\mu}k}/k^{5/2}$ (dashed line) and according to $e^{-\hat{\mu}k}$ (solid line) for two values of the temperature.

is expected, since the vanishing of $\hat{\mu}$ implies the appearance of k cycles with arbitrarily large k, i.e. cycles of permutating particles with arbitrarily large spatial extension, corresponding to a diverging correlation length; this is not possible on a finite lattice hence the dependence Eq. (24) must be valid not too close to the condensation temperature. One might wonder whether such finite size effects are also present, on the lattices used for our investigation, for higher values of T: this issue is discussed in detail in Sec. III D, where we show that this is not the case already for $T = 1.052T_c$.

We report in Table III the results for $T_{\rm BEC}$ and ν' obtained from fits limited to a temperature range $1.052 \leq T/T_c \leq 1.582$; values do not change within errors if the range is slightly changed (but not including the lowest temperature $T = 1.017T_c$). A few examples of such fits are also reported in Fig. 4. The values obtained for χ^2/d.o.f. are reasonable, taking into account that we have mixed data obtained for different values of the lattice spacing and that scaling violations, even if small, may be

TABLE II. Chemical potentials obtained for different temperatures by fitting the densities ρ_k according to $\rho_k \propto e^{-\hat{\mu}k}/k^{\alpha}$, for different values of α.

T/T_c	$\mu(\alpha = 3)$	$\mu(\alpha = 2.5)$	$\mu(\alpha = 2)$	$\mu(\alpha = 0)$
1.017[a]	0.43(4)	0.51(3)	0.61(4)	0.98(4)
1.052[b]	0.49(5)	0.58(4)	0.68(3)	1.00(4)
1.095[a]	0.75(5)	0.86(4)	1.02(4)	1.46(4)
1.168[b]	1.16(4)	1.32(4)	1.44(5)	1.96(6)
1.187[a]	1.11(6)	1.29(5)	1.36(6)	1.89(6)
1.295[a]	1.67(6)	1.85(9)	2.03(9)	2.70(15)
1.315[b]	1.89(4)	2.04(6)	2.20(8)	2.85(15)
1.424[a]	2.18(6)	2.38(6)	2.58(6)	3.4(1)
1.503[b]	2.64(10)	2.8(1)	3.0(1)	3.8(1)
1.582[a]	2.69(10)	2.9(1)	3.1(1)	3.92(8)
1.754[b]	3.16(8)	3.37(10)	3.57(10)	4.37(15)

TABLE III. Results of the fit of chemical potentials according to $\hat{\mu} = A(T - T_{\rm BEC})^{\nu'}$, for various different values of α. The lowest temperature, $T = 1.017$, has always been discarded from the fit.

α	$T_{\rm BEC}/T_c$	ν'	χ^2/d.o.f.
3	1.005(13)	0.71(5)	2.24
2.5	1.000(12)	0.68(5)	1.23
2	0.989(13)	0.68(5)	1.72
0	0.988(15)	0.61(5)	2.34

present; the ansatz given in Eq. (24) seems to work slightly better for the chemical potentials obtained in the case $\alpha = 2.5$, i.e. the value expected for free bosons.

As can be inferred from Table III, the dependence of $T_{\rm BEC}$ and ν' on the exponent α, used to deduce the chemical potentials from the densities ρ_k, is very mild or even negligible within errors. That makes the main result of our analysis stronger and less dependent on the way we deal with interactions: $T_{\rm BEC}$ is compatible within errors with the critical temperature T_c at which the SU(2) pure gauge theory deconfines. Therefore we have proved that, as we proceed from higher to lower temperatures, the onset of confinement is associated with the condensation of thermal monopoles present in the deconfined phase, as expected in the dual superconductor scenario for color confinement.

If monopole condensation indeed coincides with deconfinement, a second important question regards the relation of the critical exponent ν' with the critical exponents of the second order SU(2) deconfinement transition, which belongs to the three-dimensional (3D) Ising universality class. As clearly visible from Table III, the value obtained for ν' is compatible or slightly larger than the critical exponent related to the diverging behavior of the correlation length at the transition, $\xi \sim (T - T_c)^{-\nu}$, which for

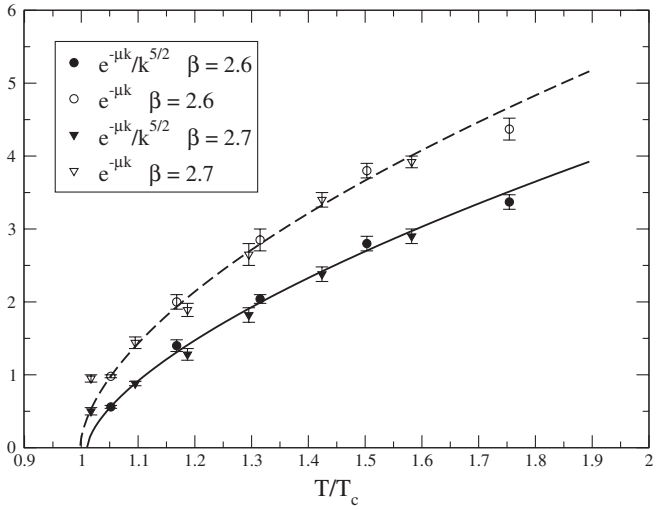

FIG. 4. Chemical potentials reported in Table II for $\alpha = 0$ and $\alpha = 2.5$ and two different lattice spacings, together with a fit of them according to Eq. (24).

Ising 3D is $\nu \sim 0.63$: in the following we shall try to give a possible interpretation of this fact.

The increase in the correlation length ξ, observed when approaching the critical condensation temperature from above, may be related to the appearance of larger and larger k cycles, corresponding to groups of permutating particles which extend over larger and larger spatial extensions. We may assume that ξ grows proportionally to the typical spatial extension of k cycles. For a distribution of k cycles $\rho_k \sim e^{-\hat{\mu}k}/k^{\alpha}$, the average value of k is $\langle k \rangle \propto 1/\hat{\mu}$; therefore, if we knew how the typical spatial extension of a k cycle depends on k, the dependence of ξ on $\hat{\mu}$ would be easily obtained. In the free boson case, the typical spatial extension of a k cycle is $\propto \sqrt{k}$, corresponding to a random walk behavior. However, the size is expected to grow faster with k because of particle-particle repulsive interactions: as a limiting case, opposite to the random walk behavior, the tyical size of a k cycle may grow linearly with k if interactions induce ordered linear structures in the set of permutating particles (e.g. the particles are typically disposed on some closed smooth line). In general we expect $\xi \propto 1/\hat{\mu}^{\omega}$, where we have introduced the exponent ω which dictates how the size of k cycles grows and is expected to be in the range $1/2 \leq \omega \leq 1$: lower values of ω could be possible if the permutating particles are more closely packed than in the noninteracting case, but this is not expected in presence of repulsive interactions. Since $\xi \sim (T - T_c)^{-\nu}$, we expect $\hat{\mu} \sim (T - T_c)^{\nu/\omega}$, hence $\nu' = \nu/\omega$.

From Table III we conclude that ν' is compatible with ν, as expected if $\omega \sim 1$: this suggests that the typical sets of permutating thermal monopoles contributing to the path integral form linearly ordered structures, which are likely induced by interactions. Therefore the typical cluster of monopole currents corresponding to a k cycle contribution should lie on a sort of time oriented closed surface (see Ref. [32] for a recent discussion about the possible appearance of similar structure right above T_c).

D. Finite size effects

As discussed above, it is natural to expect that the density of trajectories with a high wrapping number may be affected by the finiteness of the system in the spatial directions. That may be a source of systematic error in our analysis, in particular, for the temperatures closest to the transition, where the density of multiple wrapping trajectories is higher. In fact, if the typical cycle extension is really linked to the correlation length of the system, such effects are another way of looking at the saturation of ξ as the critical temperature is approached on a finite lattice. Our data have been obtained on two different combinations of lattice size and bare coupling, i.e. $L_s = 48$ at $\beta = 2.6$ and $L_s = 64$ at $\beta = 2.7$: in both cases the physical spatial size is approximately the same, $T_c L_s a(\beta) \sim 4.5$.

Therefore, in order to check for finite size effects, we have considered the lowest temperature included in our analysis, i.e. $T = 1.052 T_c$ (corresponding in our numerical setup to $\beta = 2.6$ and $N_t = 10$), where we have repeated the determination of the densities of multiple wrapping trajectories and of the chemical potential $\hat{\mu}$ on various different spatial lattice sizes, $L_s = 32$, 40, 48, 56, 64, corresponding to $T_c L_s a(\beta)$ ranging from 3 to 6.

Results obtained for the densities of multiple wrapping trajectories are reported in Table IV and in Fig. 5. In Table IV we also report the determination of the chemical potential $\hat{\mu}$ in the free boson approximation ($\alpha = 2.5$) on the different lattice sizes.

Finite size effects are clearly visible on the smallest lattice and result in a stronger suppression of trajectories with a large number of wrappings, or equivalently in a higher value of $\hat{\mu}$. However, results are compatible within errors for the three largest lattices, $L_s = 48$, 56, 64. We take that as evidence that finite size systematic effects are negligible, within our current statistical uncertainties, for spatial lattice sizes $aL_s \geq 4.5 T_C^{-1}$ and for temperatures $T \geq 1.052 T_c$. Such systematic effects therefore do not affect our analysis presented above.

TABLE IV. Normalized densities for $T = 1.052 T_c$ ($\beta = 2.60$ and $N_t = 10$) and various spatial lattices L_s. The chemical potentials obtained for $\alpha = 2.5$ are also reported. For the explorable number of wrappings, finite size effects are negligible, within errors, for $L_s \geq 48$.

	$L_s = 32$	$L_s = 40$	$L_s = 48$	$L_s = 56$	$L_s = 64$
ρ_1/T^3	0.317(4)	0.316(4)	0.315(5)	0.315(4)	0.315(5)
ρ_2/T^3	1.45(2) 10^{-2}	1.37(2) 10^{-2}	1.35(1) 10^{-2}	1.36(2) 10^{-2}	1.33(1) 10^{-2}
ρ_3/T^3	2.51(7) 10^{-3}	2.41(5) 10^{-3}	2.42(4) 10^{-3}	2.38(6) 10^{-3}	2.39(4) 10^{-3}
ρ_4/T^3	5.0(3) 10^{-4}	6.1(3) 10^{-4}	7.0(2) 10^{-4}	6.6(3) 10^{-4}	6.7(2) 10^{-4}
ρ_5/T^3	0.94(15) 10^{-4}	1.8(2) 10^{-4}	2.5(2) 10^{-4}	2.3(2) 10^{-4}	2.30(15) 10^{-4}
ρ_6/T^3	0.13(5) 10^{-4}	0.52(8) 10^{-4}	0.82(5) 10^{-4}	0.80(13) 10^{-4}	0.88(7) 10^{-4}
ρ_7/T^3	0.2(2) 10^{-5}	1.4(5) 10^{-5}	3.6(5) 10^{-5}	3.0(7) 10^{-5}	2.7(5) 10^{-5}
ρ_8/T^3	-	4(3) 10^{-6}	11(3) 10^{-6}	14(4) 10^{-6}	11(3) 10^{-6}
ρ_9/T^3	-	1(1) 10^{-6}	4(2) 10^{-6}	3(2) 10^{-6}	6(2) 10^{-6}
ρ_{10}/T^3	-	1(1) 10^{-6}	2(1) 10^{-6}	2(1) 10^{-6}	3(1) 10^{-6}
$\mu(\alpha = 2.5)$	1.25(6)	0.76(4)	0.58(4)	0.57(3)	0.56(3)

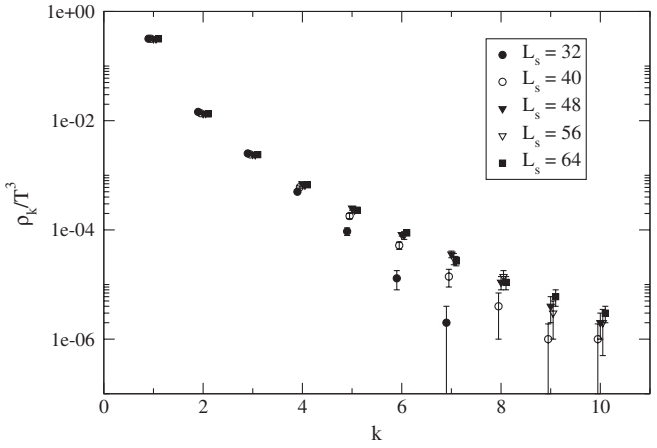

FIG. 5. Dependence of the normalized densities ρ_k/T^3 on the spatial lattice size for $\beta = 2.60$ and $N_t = 10$ ($T/T_c = 1.052$).

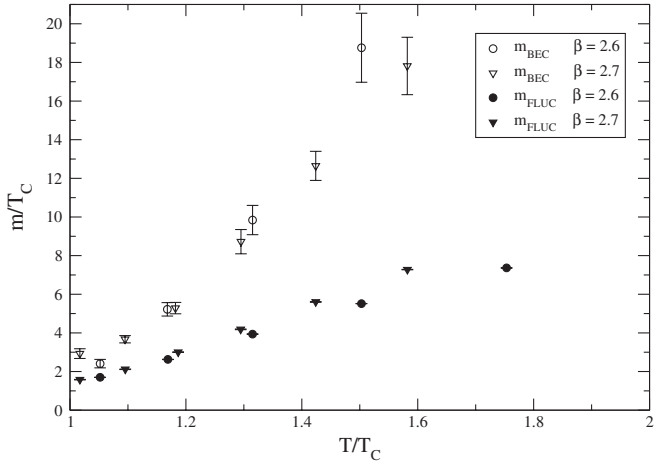

FIG. 6. Monopole masses as a function of T/T_c, as reported in Table V.

IV. MONOPOLE MASS

We have followed different strategies in order to determine a temperature dependent effective monopole mass. As we shall discuss, different definitions lead to different results, so that no unambiguous determination can be achieved; nevertheless one can identify some common features.

The first strategy is to consider the fit of the densities of wrapping trajectories ρ_k according to the nonrelativistic free boson prediction, Eq. (19), and extract from the coefficient $1/\lambda^3$ an estimate for an effective dynamical mass

$$m_{\mathrm{BEC}} = \frac{2\pi}{T\lambda^2}. \tag{25}$$

If we consider the same fits used to compute the chemical potentials reported in Table II for $\alpha = 2.5$, we obtain the masses reported in the second column of Table V and also in Fig. 6. The dependence on the lattice spacing seems negligible within errors. If we neglect the determination obtained for $T = 1.017T_c$, where as discussed in previous section finite size effects could be significant, we see a clear trend for an effective monopole mass rapidly decreasing from values of the order of $20T_c$ for $T \sim 1.5T_c$ down to $m_{\mathrm{BEC}} \sim T_c$ at T_c. Of course, when m_{BEC} is of the order of T_c the nonrelativistic approximation breaks down, however even a linear fit taking into account only values for $T \geq 1.095T_c$, where m_{BEC} is already a few times T_c and relativistic corrections can be neglected, leads to predict $m_{\mathrm{BEC}} \sim T_c$ at the transition.

TABLE V. Monopole masses, determined for different temperatures according to the definitions given in Eqs. (25) and (28).

T/T_c	m_{BEC}/T_c	m_{FLUC}/T_c
1.017[a]	2.93(25)	1.56(1)
1.052[b]	2.41(22)	1.71(1)
1.095[a]	3.67(19)	2.15(1)
1.168[b]	5.22(35)	2.62(1)
1.187[a]	5.28(29)	3.00(2)
1.295[a]	8.72(63)	4.18(2)
1.315[b]	9.84(76)	3.93(1)
1.424[a]	12.6(8)	5.63(2)
1.503[b]	19(2)	5.53(1)
1.582[a]	18(2)	7.29(2)
1.754[b]	25(3)	7.36(1)

A different strategy is to relate the monopole mass to the spatial fluctuations of monopole trajectories: those should be more and more damped as the mass increases. Consider again the path integral of a nonrelativistic particle of mass m and the average squared spatial fluctuation of the particle periodic path, defined as

$$\Delta x^2 \equiv T \int_0^{1/T} dt \langle (\vec{x}(t) - \vec{x}(0))^2 \rangle, \tag{26}$$

where the average is taken over the path integral distribution. That is directly related to the mass of the particle. A simple calculation shows that for a free nonrelativistic particle one has $\Delta x^2 = 1/(2mT)$, while for a particle in a harmonic potential with elastic constant $m\omega^2$, one obtains $\Delta x^2 = -6/(\beta m\omega^2) + 3\coth(\omega\beta/2)/(m\omega)$.

On the lattice the mean squared monopole fluctuation is defined as

$$a^{-2}\Delta x^2 = \frac{1}{L}\sum_{i=1}^{L} d_i^2, \tag{27}$$

where d_i is the squared spatial distance (accounting for periodical boundary conditions) between the starting site of the monopole current at $t = 0$ and the current position after i steps along the monopole trajectory, while L is the total length of the trajectory (all quantities measured in lattice spacing units). We have measured this quantity on trajectories wrapping only one time and tried to relate it to the monopole mass. We have considered the free particle

approximation, thus defining a mass

$$m_{\mathrm{FLUC}} = \frac{1}{2T\Delta x^2}, \tag{28}$$

and obtaining the results reported in Table V and in Fig. 6. A better approximation would be to consider interactions at a mean field level. One can take the charge distribution around a monopole from the correlation function $g(r)$ computed in Ref. [8] and determine the potential around the position of a monopole induced by nearby monopoles and antimonopoles, then approximating it by an attractive harmonic potential: we have tried this procedure obtaining negligible corrections to the free particle approximation.

The mass obtained in this way shows some scaling deviations, especially at high T, which can be explained as follows. Wrapping monopole trajectories are not strict one-dimensional lines as in the one-particle path integral, but have some finite thickness, part of which is due to unphysical ultraviolet fluctuations in the form of monopole-antimonopole loops at the scale of the UV cutoff, which may be attached to a physical wrapping trajectory. Such unphysical fluctuations add to the physical ones that we are investigating. It is not easy to give a definition for a proper subtraction of the unphysical contribution. However, we notice that it becomes negligible close to T_c, where physical fluctuations of the trajectory become important: that is signalled by the fact that scaling is better and better as we approach T_c.

The value of the monopole mass obtained from spatial fluctuations of trajectories differs significantly from that obtained in the BEC approach: that is expected since m_{BEC} is related to the properties of multiple wrapping trajectories, while m_{FLUC} to those of single wrapping trajectories: in both cases we have relied on some effective free particle behavior, but consistent results would have been obtained only if the particles were really free. It is however remarkable that also m_{FLUC} decreases rapidly as the transition temperature is approached, getting compatible with m_{BEC} if extrapolated down to T_c (see Fig. 6).

TABLE VI. Average squared fluctuations measured as reported in Eq. (27), as a function of T/T_c, for trajectories having wrapping numbers $k = 1, 2, 3$.

T/T_c	$T^2\Delta x^2_{k=1}$	$T^2\Delta x^2_{k=2}$	$T^2\Delta x^2_{k=3}$
1.017[a]	0.322(6)	1.85(3)	3.16(6)
1.052[b]	0.309(2)	1.73(2)	3.10(3)
1.095[a]	0.259(4)	1.46(3)	2.71(7)
1.168[b]	0.222(1)	1.23(2)	2.42(5)
1.187[a]	0.198(1)	1.58(2)	2.06(6)
1.295[a]	0.155(1)	0.92(2)	1.90(13)
1.315[b]	0.1670(7)	0.915(12)	1.80(6)
1.424[a]	0.1271(5)	0.741(8)	1.50(7)
1.503[b]	0.1362(4)	0.722(6)	1.45(6)
1.582[a]	0.1087(3)	0.656(9)	1.23(7)
1.754[b]	0.1109(3)	0.616(8)	1.30(8)

Finally, let us comment on Δx^2 measured on trajectories wrapping more than one time. In Table VI we report the values of $T^2\Delta x^2(k)$ measured for $k = 1, 2, 3$ at various temperatures. In the case of free particles one would expect $\Delta x^2(k) \sim k\Delta x^2(k = 1)$, instead, as anticipated in Sec. III C, values increase faster with k because of monopole-monopole repulsions. In particular $\Delta x^2(k = 2)$ and $\Delta x^2(k = 3)$ are, respectively, about 5–6 times and 10 times larger than $\Delta x^2(k = 1)$.

V. DISCUSSION AND CONCLUSIONS

Let us summarize the main results obtained in this work. We have considered the statistical distribution in the number of wrappings in the Euclidean time direction, for thermal monopole trajectories exposed after MAG Abelian projection in the deconfined phase of SU(2) pure gauge theory. We have shown that such distribution is compatible with that of a Bose gas condensing exactly at the confinement/deconfinement critical temperature T_c of the pure gauge theory. This result represents a strong link between confinement, monopole condensation, and thermal monopoles. We have also found that in the approach to the criticality in the monopole ensemble, as T decreases to T_c from above, the monopole masses are significantly reduced, and their interactions weaken. That fits into the overall idea of plasma gradually switching from electric to magnetic one. Our quantitative results about cluster densities shed further light on properties and interactions of the objects we call monopoles. Our investigation leaves some aspects that should be better understood and clarified and that we partially discuss in the following.

(1) The definition of monopoles studied in this work is strictly linked to a particular choice of Abelian projection, namely, to that performed in maximal Abelian gauge, so that one should understand why some other Abelian projections give different, unphysical results. Apart from usual arguments in support of MAG projection, which are based on Abelian dominance, we point out recent results, according to which the MAG projection is part of a restricted class of Abelian projections which correctly expose the magnetic content of gauge configurations [33]. However, one should be aware of the problems which, even within the MAG gauge, are related to the choice of the Gribov copy along the gauge orbit: indeed the study of Ref. [8] has shown that, while a random choice of the local maximum leads to the correct scaling to the continuum of the monopole density, different choices, even if getting closer to the global maximum (e.g. starting from a Landau gauge fixed configuration), may change the outcome[4]: this aspect must be considered more deeply in the future.

[4]Preliminary qualitative indications, following those of Ref. [8], are that, as an higher maximum is reached, a reduction of the observed densities applies more or less proportionally to the densities of each k cycle.

(2) Assuming that MAG projection identifies the correct objects, what non-Abelian gauge configurations are associated with Abelian monopoles and what is their exact physical nature? What other quantum numbers do they carry? Some steps have been done in Ref. [11], where it has been shown that a clear correlation exists between the non-Abelian gauge action density and the locations of thermal monopole trajectories; moreover, the excess of magnetic action found around monopoles is compatible with that of the electric one, so that the evidence of Ref. [11] is that thermal Abelian monopoles may be associated with topological defects carrying both electric and magnetic charge. Indeed, objects identified by MAG projection have magnetic charge, yet various other quantum numbers are in principle possible. They can in principle be just monopoles, or dyons, or (in simulations with several quark flavors) they may also have various flavors, due to binding to quark-antiquark pairs or single quarks, or be a complicated mixture of all of them. Examples of fermionic excitations possessing magnetic charge and spin $1/2$ are well known, and in fact required in any supersymmetric theory, complementing all monopole multiplets. Seiberg-Witten $\mathcal{N} = 2$ superconformal theories with matter have not only magnetic monopoles with certain flavor allocations, but they also have intricate structure of dualities, relating several different (mutually dual) Lagrangians with the same theory. So, in simulations with quarks, one would need to separate Bose and Fermi-like behavior of various magnetic objects, which is by no means trivial. Those studies, as well as other issues related with the quest for understanding of the precise spectroscopy of the magnetic sector, will hopefully be continued elsewhere.

(3) While the statistical distribution of wrappings strongly suggests the presence of a BEC-like phenomenon associated with confinement, a clear description of the physical properties of the system has not yet been achieved. The ensemble of thermal monopoles is strongly interacting and its properties resemble those of a liquid [8,9], therefore one should not try to fit its properties with those of a weakly interacting but rather with those of a strongly interacting Bose gas, like ^{4}He [25]. The effect of interactions is clearly visible in the typical shape of ''polymers'' made up of monopoles belonging to the same k cycle: we have not studied that in detail yet, but just remarked that from the scaling of the chemical potential we predict smooth linear shapes rather than the random walk behavior expected in the case of free particles; further investigation on this side could clarify more universal properties of the system.

(4) Another peculiarity of the system is that in fact it is a plasma of monopoles and antimonopoles with Coulomb-like screened interactions, i.e. it resembles a Bose-Coulomb gas system which is neutral on average: in this sense the chemical potential that we have introduced in our analysis should not be regarded as a true chemical potential, but rather as a parameter entering an effective description of the increase in the number of k cycles.

(5) The vanishing of the chemical potential $\hat{\mu}$ at the transition, with a critical exponent ν' [see Eq. (24)] compatible with the 3D Ising critical exponent ν of the correlation length, shows that $\hat{\mu}$ scales with the same critical behavior of a mass. It would be interesting to better understand the meaning of this in the future, for instance by investigating the relation between the distribution in the number of wrappings of monopole trajectories and other quantities of dual nature, showing a critical behavior above T_c, like the dual string tension related to the spatial 't Hooft loop [34–36].

(6) The fact that we still do not have a consistent physical description of the system manifests itself, for instance, in the absence of a consistent definition of effective monopole mass. However, it is interesting to notice that different definitions tend to a common value $m \sim T_c$ when the condensation temperature is approached, where they are also roughly in agreement with the estimates reported in Ref. [25]. A similar physical scale comes out when studying the electric-magnetic asymmetry in Landau gauge [37]: it would be important to understand if the two scales are connected in some way.

(7) The fact that we obtain a condensation temperature $T_{\mathrm{BEC}} = T_c$, within our statistical uncertainties, by just extrapolating data for the densities of trajectories with multiple wrappings, may be peculiar to SU(2) pure gauge theory, where the confinement/deconfinement transition is of second order nature; hence there is a critical behavior at the transition. In different cases, like for a first order transition, hence e.g. for the SU(3) pure gauge theory, while one expects monopole condensation to happen at T_c anyway, the statistical analysis of the distribution of wrapping trajectories above T_c could point to a condensation temperature slightly below the actual deconfinement temperature, i.e. to a sort of spinodal point. In this sense SU(2) pure gauge theory is a system where the connection between confinement and monopole condensation can be better established. We would like to clarify this point in the future by extending our investigation to SU(3) color gauge group, with and without dynamical quark contributions.

ACKNOWLEDGMENTS

We thank the organizers of the workshop ''Non-Perturbative Methods in Strongly Coupled Gauge Theories'' at the Galileo Galilei Institute (GGI) in Florence, where this work has been started. We thank D. Antonov, C. M. Becchi, M. Chernodub, M. Cristoforetti, A. Di Giacomo, P. de Forcrand, M. Ilgenfritz, J. Liao, E. Vicari, and V. Zakharov for useful discussions. Numerical simulations have been performed on GRID resources provided by INFN.

[1] G. 't Hooft, *EPS International Conference on High Energy Physics, Palermo, 1975*, edited by A. Zichichi (Ed. Compositori, Bologna, Italy, 1975).
[2] S. Mandelstam, Phys. Rep. **23**, 245 (1976).
[3] J. Liao and E. Shuryak, Phys. Rev. C **75**, 054907 (2007).
[4] M. N. Chernodub and V. I. Zakharov, Phys. Rev. Lett. **98**, 082002 (2007); arXiv:hep-ph/0702245.
[5] E. Shuryak, Prog. Part. Nucl. Phys. **62**, 48 (2009).
[6] V. G. Bornyakov, V. K. Mitrjushkin, and M. Muller-Preussker, Phys. Lett. B **284**, 99 (1992).
[7] S. Ejiri, Phys. Lett. B **376**, 163 (1996).
[8] A. D'Alessandro and M. D'Elia, Nucl. Phys. **B799**, 241 (2008).
[9] J. Liao and E. Shuryak, Phys. Rev. Lett. **101**, 162302 (2008).
[10] C. Ratti and E. Shuryak, Phys. Rev. D **80**, 034004 (2009).
[11] M. N. Chernodub, A. D'Alessandro, M. D'Elia, and V. I. Zakharov, arXiv:0909.5441.
[12] M. Lublinsky, C. Ratti, and E. Shuryak, Phys. Rev. D **81**, 014008 (2010).
[13] A. Di Giacomo, B. Lucini, L. Montesi, and G. Paffuti, Phys. Rev. D **61**, 034503 (2000); **61**, 034504 (2000).
[14] J. M. Carmona, M. D'Elia, A. Di Giacomo, B. Lucini, and G. Paffuti, Phys. Rev. D **64**, 114507 (2001).
[15] J. M. Carmona, M. D'Elia, L. Del Debbio, A. Di Giacomo, B. Lucini, and G. Paffuti, Phys. Rev. D **66**, 011503 (2002).
[16] M. D'Elia, A. Di Giacomo, B. Lucini, G. Paffuti, and C. Pica, Phys. Rev. D **71**, 114502 (2005).
[17] M. N. Chernodub, M. I. Polikarpov, and A. I. Veselov, Phys. Lett. B **399**, 267 (1997).
[18] P. Cea and L. Cosmai, J. High Energy Phys. 11 (2001) 064; P. Cea, L. Cosmai, and M. D'Elia, J. High Energy Phys. 02 (2004) 018.
[19] A. D'Alessandro, M. D'Elia, and L. Tagliacozzo, Nucl. Phys. **B774**, 168 (2007).
[20] S. Conradi, A. D'Alessandro, and M. D'Elia, Phys. Rev. D **76**, 054504 (2007).
[21] R. P. Feynman, Phys. Rev. **90**, 1116 (1953).
[22] R. P. Feynman, Phys. Rev. **91**, 1291 (1953).
[23] V. Elser, Ph.D. thesis, University of California Berkeley, 1984.
[24] D. M. Ceperley, Rev. Mod. Phys. **67**, 279 (1995).
[25] M. Cristoforetti and E. Shuryak, Phys. Rev. D **80**, 054013 (2009).
[26] S. Ito, S. Kato, K. I. Kondo, T. Murakami, A. Shibata, and T. Shinohara, Phys. Lett. B **645**, 67 (2007).
[27] A. D'Alessandro and M. D'Elia, Proc. Sci., CONFINEMENT8 (2008) 127.
[28] A. De Grand and D. Toussaint, Phys. Rev. D **22**, 2478 (1980).
[29] P. Cea and L. Cosmai, Phys. Rev. D **52**, 5152 (1995).
[30] J. Engels, F. Karsch, and K. Redlich, Nucl. Phys. **B435**, 295 (1995).
[31] J. Fingberg, U. Heller, and F. Karsch, Nucl. Phys. **B392**, 493 (1993).
[32] M. N. Chernodub, A. Nakamura, and V. I. Zakharov, arXiv:0904.0946.
[33] C. Bonati, A. Di Giacomo, L. Lepori, and F. Pucci, arXiv:1002.3874 [Phys. Rev. D (to be published)].
[34] G. 't Hooft, Nucl. Phys. **B138**, 1 (1978).
[35] C. Korthals-Altes, A. Kovner, and M. A. Stephanov, Phys. Lett. B **469**, 205 (1999).
[36] P. de Forcrand, M. D'Elia, and M. Pepe, Phys. Rev. Lett. **86**, 1438 (2001).
[37] M. N. Chernodub and E. M. Ilgenfritz, Phys. Rev. D **78**, 034036 (2008).